HHS Public Access

Author manuscript

Hypertension. Author manuscript; available in PMC 2019 August 01.

Published in final edited form as:

Hypertension. 2018 August ; 72(2): 370–380. doi:10.1161/HYPERTENSIONAHA.118.11239.

Angiotensin II-induced end organ damage in mice is attenuated by human exosomes and by an exosomal Y RNA fragment

Linda Cambier[1,2], **Jorge F. Giani**[2], **Weixin Liu**[1], **Takeshi Ijichi**[1], **Antonio K. Echavez**[1], **Jackelyn Valle**[1], and **Eduardo Marbán**[1]

[1]Smidt Heart Institute, Cedars-Sinai Medical Center, 8700 Beverly Blvd., Los Angeles, CA, 90048, USA

[2]Department of Biomedical Sciences, Cedars-Sinai Medical Center, 8700 Beverly Blvd., Los Angeles, CA, 90048, USA

Abstract

Hypertension often leads to cardiovascular disease (CVD) and kidney dysfunction. Exosomes secreted from cardiosphere-derived cells (CDC-exo) and their most abundant small RNA constituent, the Y RNA fragment EV-YF1, exert therapeutic benefits after myocardial infarction. Here, we investigated the effects of CDC-exo and EV-YF1, each administered individually, in a model of cardiac hypertrophy and kidney injury induced by chronic infusion of angiotensin (Ang) II. After 2 weeks of Ang II, multiple doses of CDC-exo or EV-YF1 were administered retro-orbitally. Ang II infusion induced an elevation in systolic blood pressure that was not affected by CDC-exo or EV-YF1. Echocardiography confirmed that Ang II infusion led to cardiac hypertrophy. CDC-exo and EV-YF1 both attenuated cardiac hypertrophy and reduced cardiac inflammation and fibrosis. In addition, both CDC-exo and EV-YF1 improved kidney function, and diminished renal inflammation and fibrosis. The beneficial effects of CDC-exo and EV-YF1 were associated with changes in the expression of the anti-inflammatory cytokine IL-10 in plasma, heart, spleen and kidney. In summary, infusions of CDC-exo or EV-YF1 attenuated cardiac hypertrophy and renal injury induced by Ang II infusion, without affecting blood pressure, in association with altered IL-10 expression. Exosomes and their defined noncoding RNA contents may represent potential new therapeutic approaches for hypertension-associated cardiovascular and renal damage.

Keywords

CDC-exosomes; EV-YF1; IL-10; hypertrophy; kidney; macrophage; angiotensin II

Corresponding Author: Eduardo Marbán, MD, PhD, 8700 Beverly Blvd,, Los Angeles, CA, 90048, Phone: 310-423-7557, Fax: 310-423-7637, Eduardo.Marban@cshs.org.

Disclosures

EM owns founders' equity in Capricor, Inc. No conflicts of interest, financial or otherwise, are declared by the other authors.

Author contributions

LC established the hypotheses, designed the study, performed experiments, analyzed data, and wrote the manuscript. JFG assisted with data collection and analysis, design of the study, and writing the manuscript. AE helped in surgical animal procedures. WL, TI and JV provided technical assistance. EM established the hypotheses, designed the study, co-analyzed data, and revised the manuscript. All authors read and approved the final version of the manuscript.

Introduction

Cardiovascular disease (CVD) is estimated to affect 92.1 million adults in the US. By 2030, almost half of the US adult population is projected to have some form of CVD.[1] Risk factors implicated in CVD include lifestyle (tobacco use, physical inactivity, nutrition), high blood pressure, metabolic syndrome and genetics. In response to CVD, the heart often undergoes a compensatory response known as maladaptive hypertrophy,[2] increasing the size of preexisting cardiomyocytes. The left ventricle (LV) undergoes biochemical, structural and metabolic changes to maintain cardiac function.[3, 4] Such cardiac remodeling is accompanied by inflammation, fibrosis and apoptosis which lead to ventricular dilation, contractile dysfunction, and eventually, progression to heart failure (HF).[5] CVD and kidney dysfunction often go hand in hand, ultimately leading to the failure of both organs. In patients with chronic kidney disease, HF is the major cardiovascular complication and its prevalence increases with declining kidney function.[6]

Cardiosphere-derived cells (CDCs)[7] are cardiac progenitor cells which have been tested in humans for myocardial infarction, Duchenne muscular dystrophy and other indications.[8–12] These cells improve tissue repair via their anti-apoptotic, anti-fibrotic, anti-remodeling, angiogenic and cardioproliferative characteristics. They also promote cardioprotection by modulating the inflammatory response.[13] CDCs work indirectly when applied *in vivo*: their effects are mediated via secreted exosomes (CDC-exo), lipid-bilayer vesicles 30-150 nm in diameter.[14] Exosomes carry a unique cargo of lipids, proteins, and RNAs, which only partially reflect the cell of origin. We have previously reported that the most prevalent species in CDC-exo, after tRNAs, are Y RNAs and their fragments, which constitute almost 20% of the total small exosomal RNAs.[15] Y RNAs are non-coding RNAs, first discovered in 1981 in the serum from patients suffering from autoimmune diseases, complexed with the ribonucleoproteins Ro60 and La.[16, 17] Humans possess four Y-RNA genes (hY1, hY3, hY4 and hY5 RNA).[18] The complex Ro-Y RNA has been implicated in RNA processing and quality control of non-coding RNA.[19] A role in the initiation step of chromosomal DNA replication has also been attributed to Y-RNAs, independent of Ro60 or La association.[20] Recently, a plethora of deep sequencing studies in eukaryotes have identified small RNA fragments derived from longer RNAs.[21] Accumulating evidence suggests that these RNA fragments, while derived from pre-existing non-coding RNAs, may themselves be bioactive.[22] Moreover, Y-RNA fragments comprise a substantial fraction of the RNA component of exosomes present in many physiological fluids[23] and cell types[24]. The function of extracellular Y-RNA fragments is currently unknown, but it has been speculated that they are processed and secreted as part of an as-yet undefined signaling process.[25] The most abundant individual small RNA present in CDC-exo is a 56-nucleotide fragment of Y4 RNA, EV-YF1, which confers cardioprotection via modulation of IL-10 expression and secretion.[15]

Here, we explored whether EV-YF1 and CDC-exo exert beneficial effects in a model of cardiac hypertrophy and kidney injury induced by chronic infusion of angiotensin (Ang) II.[26–28] Inflammation plays a critical role in the pathogenesis of Ang II-induced heart and renal injury,[29, 30] and the anti-inflammatory effects of IL-10 have been shown to play a protective role in this model of CVD.[27] We demonstrate that EV-YF1 largely recapitulates the effects

of CDC-exo by attenuating maladaptive cardiac hypertrophy and improving kidney function, without altering blood pressure. These benefits are associated with enhanced IL-10 secretion.

Methods

The authors declare that all supporting data are available within the article and online-only Data Supplement.

Animals

Eight to ten-week-old male C57BL/6J mice were obtained from Jackson Laboratories. Hypertension was induced with subcutaneous Ang II infusion (1.4 mg/kg/day) (Sigma-Aldrich, St. Louis, MO, USA) using osmotic mini-pumps (Alzet, Cupertino model 1004, CA, USA) for 28 days. The Institutional Animal Care and Use Committee approved all animal care and related procedures before study commencement.

CDCs, exosomes and EV-YF1

Human CDCs were isolated and cultured, and exosomes isolated, as described.[14, 31] EV-YF1 was synthesized commercially from Integrated DNA Technologies (IDT) (Coralville, IA).

Statistics

Results are expressed as mean ± SEM. Groups were compared using 1-way ANOVA followed by Tukey's multiple comparisons test. *$p < 0.05$, **$p < 0.01$, ***$p < 0.001$. All analyses were performed using Prism 5 software (GraphPad).

Detailed methods are provided in the online-only Data Supplement.

Results

EV-YF1 and CDC-exo biodistribution after retro-orbital injection in Ang II-infused mice

To investigate the role of EV-YF1 and CDC-exo during cardiac hypertrophy and renal injury, we used the Ang II-induced hypertension model.[26–28] LV hypertrophy was induced in C57BL/6J mice by subcutaneous infusion of Ang II (1.4 mg/kg/day) using osmotic mini-pumps for 28 days. Sham animals were infused with saline solution. On days 14, 15, 18, 20 and 22 of Ang II infusion, animals were treated with consecutive doses of EV-YF1 synthetic oligoribonucleotide, CDC-exo or saline by retro-orbital injection (Figure 1A). To determine the efficacy of retro-orbital injection, expression of EV-YF1 was analyzed 24 h after a single injection of the EV-YF1 synthetic oligoribonucleotide or CDC-exo. Although EV-YF1 is highly abundant in CDC-exo,[15] the dose of synthetic oligoribonucleotide (4.79E+14 copies) injected likely exceeds the abundance of EV-YF1 delivered in CDC-exo. Indeed, we observed more expression of EV-YF1 after EV-YF1 injection than CDC-exo injection in all tested organs with higher copy numbers in heart, spleen and liver. Similar expression levels of EV-YF1 were observed in lung and kidneys, but no expression was detected in brain (Figure 1B). While CDC-exo biodistribution shows some predilection for the heart[31], possibly because of CDC-exo surface protein composition, we have not yet investigated the

mechanism of biodistribution of EV-YF1. Clearly the observed pattern does not follow linearly the relative perfusion of the various organs[32]: heart and spleen are disproportionately rich in EV-YF1, while lung, brain and kidney are low relative to blood flow. To confirm the hypertensive effect of Ang II, we measured systolic blood pressure (SBP) before (day 0) and weekly during Ang II infusion. After one week of Ang II, SBP increased significantly compared to the sham group infused with saline (135±6 vs. 107±5 mmHg, n=5). This increase persisted during the 4 weeks of infusion. Neither the administration of EV-YF1 nor CDC-exo altered blood pressure levels (Figure 1C).

Effects of EV-YF1 and CDC-exo on cardiac function and hypertrophy

Echocardiography revealed no differences in LV systolic (Figure S1A and S1B in the online-only Data Supplement) or diastolic (Figure S1C in the online-only Data Supplement) function after Ang II infusion with or without EV-YF1 or CDC-exo. However, LV posterior wall dimension in end-diastole was greater after 4 weeks of Ang II infusion compared to sham (1.5 ± 0.1 vs. 0.84 ± 0.06 mm, $p < 0.01$, n =3-6). The augmented thickness was significantly blunted in the CDC-exo group (1.05 ±0.07 mm; $p<0.01$, n=6). No improvement of LV posterior wall thickness was observed in the EV-YF1 group (1.34 ± 0.09 mm, p=0.6, n=6) (Figure 2A; Figure S1D in the online-only Data Supplement). The decrease in LV internal diastolic diameter induced by Ang II-infusion (Sham: 3.4 ± 0.2; Ang II: 2.5 ± 0.1 mm, $p<0.05$, n=4-5) was less pronounced in CDC-exo group (3.2 ± 0.11 mm, $p<0.05$ vs. Ang II, n=6). EV-YF1 also blunted the decrease in LV internal diameter induced by Ang II, albeit not significantly (3.0 ± 0.1 mm vs. Ang II, p=0.2) (Figure 2B; Figure S1D in the online-only Data Supplement). No differences in interventricular septal thickness in end-diastole were observed between groups (Figure 2C; Figure S1D in the online-only Data Supplement), but LV mass showed a significant increase in the Ang II-infused group (137 ± 5 mg vs sham 102 ± 6 mg, $p<0.05$, n=5). This augmentation in mass was reduced in both EV-YF1 (94 ± 8 mg, $p<0.01$, n=8) and CDC-exo (87.7 ± 4.6 mg, $p<0.001$, n=8) groups (Figure 2D). The heart/body weight ratio, indicative of cardiac hypertrophy, mimicked the profile obtained for corrected LV mass (Figure 2E). To analyze this parameter, administration of the scrambled oligoribonucleotide of EV-YF1, Ys, in a group of animals infused with Ang II was added and no difference was observed between this group and the Ang II group (Figure S2A online-only Data Supplement). Another characteristic of cardiac hypertrophy is the re-expression of fetal genes such as *Anp*. Indeed, *Anp* expression was 5.7-fold greater in Ang II-infused compared to sham group ($p<0.001$, n=6) while the induction was only 3.6 and 2.6-fold in EV-YF1 and CDC-exo groups; ($p<0.01$ and $p<0.001$ vs. Ang II-infused group; respectively, n=6-5) (Figure 2F). Taken together, these data indicate that both EV-YF1 and CDC-exo attenuated cardiac hypertrophy induced by Ang II infusion for 4 weeks. Some parameters of LV hypertrophy were less improved by EV-YF1 than by CDC-exo, but the “gold standard” measures of LV mass and heart/body weight ratio were affected comparably by the two interventions.

EV-YF1 and CDC-exo decrease Ang II-induced cardiac hypertrophy, fibrosis and inflammation

LV remodeling during cardiac hypertrophy is characterized by an increase in cardiomyocyte size, cardiac fibrosis and inflammation. Cardiomyocyte cross-sectional area was increased in

Ang II-infused group (240 ± 23 μm^2) compared to sham (161 ± 12 μm^2, $p<0.05$, n=4); this increase was significantly attenuated in EV-YF1 and CDC-exo groups (171 ± 9 and 171 ± 15 μm^2, $p<0.05$ vs. Ang II group; respectively, n=4) (Figure 3A and 3B). Interstitial cardiac fibrosis was also increased by Ang II infusion (Ang II: 14 ± 3 % vs. Sham: 3.2 ± 0.8 % of area, $p< 0.01$, n=3) while EV-YF1 and CDC-exo groups showed attenuated fibrosis (EV-YF1: 5.9 ± 0.7%, $p<0.05$, n=3 and CDC-exo: 8.24 ± 2%, p=0.137 vs. Ang II mice, n=3) (Figure 3C and 3D). Inflammation was determined by analyzing the expression of *CD68* and F4/80, markers of infiltrating inflammatory cells, as well as expression of pro-inflammatory cytokines *Il6* and *Il1b*, in heart tissue. EV-YF1 and CDC-exo significantly reduced the expression of those markers in Ang II-infused animals, providing further evidence of an anti-inflammatory effect (Figure 3E and 3F; Figure S3 in the online-only Data Supplement).

EV-YF1 inhibits Ang II effects on cardiomyocytes and cardiac fibroblasts

We have shown that EV-YF1 modulates macrophage activity[15]. Here, we tested if EV-YF1 inhibits the effects of Ang II via a similar mechanism. Neonatal rat ventricular cardiomyocytes (NRVMs) were cultured for 24 h with non-conditioned media (control) or media conditioned for 48 hours by bone marrow-derived macrophages (BMDMs) overexpressing Ys scrambled oligoribonucleotide (Ys-CM) or EV-YF1 (EV-YF1-CM) with or without Ang II (1μM). In the presence of Ang II, *Anp* expression increased 1.5-fold in NRVMs cultured with control media vs. no Ang II. A similar increase (2-fold) was observed in NRVMs cultured in Ys-CM in the presence of Ang II. On the contrary, the increase in *Anp* expression induced by Ang II was significantly blunted in NRVMs cultured in EV-YF1-CM. This effect was attributable to IL-10 present in EV-YF1-CM, as inclusion of an anti-IL-10 neutralizing antibody abrogated the decrease in *Anp* expression (Figure S4A in the online-only Data Supplement). These data are consistent with the notion that, upon overexpression of EV-YF1, BMDMs secrete cytokines, including IL-10[15], that inhibit the effect of Ang II on NRVM *Anp* expression. The role of EV-YF1 on Ang II inhibitory effect via macrophages was also tested in neonatal cardiac fibroblasts (neoCFs). NeoCFs were cultured for 16 h with BMDM media (control) or media conditioned over 72 h by BMDMs overexpressing Ys (Ys-CM) or EV-YF1 (EV-YF1-CM) with or without Ang II (100 nM). Adult cardiac fibroblasts (CFs) have been shown to produce low levels of IL-6, which increase in the presence of Ang II or in co-culture with macrophages.[33] In our experiment, *Il6* expression was not increased in the presence of Ys-CM, EV-YF1-CM or Ang II alone, possibly due to the use of neonatal vs adult CFs. However, a significant increase (2.2-fold, $p<0.001$) in *Il6* expression was observed when neoCFs were cultured with conditioned media from BMDMs overexpressing Ys (Ys-CM) with Ang II. In contrast, when neoCFs were cultured with media from BMDMs overexpressing EV-YF1 (EV-YF1-CM) with Ang II, *Il6* expression was not different from the conditioned media without Ang II (Figure S4B in the online-only Data Supplement). Direct overexpression of EV-YF1 in neoCFs exposed to Ang II did not change *Il6* expression (data not shown). Thus, EV-YF1 acts on BMDMs to inhibit *Il6* induction by Ang II in neoCFs.

EV-YF1 and CDC-exo decrease Ang II-induced kidney injury

Chronic activation of the renin-angiotensin system (RAS) increases blood pressure, and leads to progressive kidney injury and proteinuria. Accordingly, we analyzed whether EV-

YF1 and/or CDC-exo exert renoprotective effects. Proteinuria was significantly increased after 4 weeks of Ang II infusion compared to saline infusion (Sham: 13 ± 1 vs. Ang II: 48 ± 4 mg/day, $p<0.001$, n=4). In EV-YF1 and CDC-exo groups, proteinuria was decreased compared to Ang II group (29 ± 4 and 31 ± 3 mg/day, $p<0.05$, n=4; respectively; Figure 4A). To analyze this parameter, administration of the scrambled oligoribonucleotide of EV-YF1, Ys, in a group of animals infused with Ang II was added and no difference was observed between this group and the Ang II group (Figure S2B in the online-only Data Supplement). Kidney levels of neutrophil gelatinase associated lipocalin (NGAL), a biomarker of renal injury,[34] tended to increase after 4 weeks of Ang II infusion compared to sham, while EV-YF1 and CDC-exo groups showed significant decreases compared to Ang II-infused group (Ang II: 2184 ± 518 vs. EV-YF1: 1261 ± 94 and CDC-exo: 1058 ± 25 pg/mg total kidney protein, $p<0.05$, n=4). These data reveal that EV-YF1 and CDC-exo ameliorate the renal injury induced by Ang II infusion (Figure 4B). To quantify glomerular injury, we evaluated structural changes histologically using periodic acid-Schiff staining. Mesangial expansion was significantly higher in Ang II-infused mice compared to control mice (Sham: 12 ± 2 vs. Ang II: 19 ± 1 % of total glomerular area, $p<0.05$; n=5; Figure 4C and 4D). On the other hand, both EV-YF1 and CDC-exo groups showed mesangial areas that were indistinguishable from those in control mice. Glomerular size was significantly decreased in Ang II-infused mice compared to control mice (Sham: 4692 ± 151 vs. Ang II: 4111 ± 176 μm^2, $p<0.05$, n=5, Figure 4E). In EV-YF1 group, glomerular size was increased, reaching values comparable to sham (4540 ± 93 μm^2). No restoration of glomerular size was observed in CDC-exo group, and no change in the number of glomeruli was observed in any experimental group (Figure S5 in the online-only Data Supplement).

EV-YF1 and CDC-exo decrease Ang II-induced renal inflammation and fibrosis

Ang II-induced hypertension is associated with an increase of infiltrating macrophages in the kidney and a consequent elevation of intrarenal cytokines, which facilitates the progression of hypertension and kidney injury.[35] To test whether EV-YF1 or CDC-exo could attenuate Ang II-induced inflammation, we analyzed the expression of *CD68*, a marker of infiltrating cells, in renal tissue. *CD68* was decreased in EV-YF1 and CDC-exo groups compared to Ang II group (Figure 5A). We also analyzed the expression levels of pro-inflammatory cytokines *Il6* and *Il1b*. Here, the differences were not significant, but a trend was observed in favor of a decrease in *Il1b* expression in both intervention groups compared to Ang II alone, along with a tendency for EV-YF1 to decrease *Il6* expression (Figure 5B and 5C). Further assessment of renal injury was performed by Masson's trichrome staining to evaluate fibrosis. Renal cortices revealed increased tubulointerstitial fibrosis in Ang II-infused mice compared to controls (Sham: 0.19 ± 0.03% vs. Ang II: 0.4 ± 0.1% of total cortical area; $p<0.01$; n=5; Figure 5D and 5E). Interestingly, EV-YF1 significantly decreased renal interstitial fibrosis (0.23 ± 0.03%, $p<0.05$ compared to Ang II group). CDC-exo also decreased renal fibrosis (0.30 ± 0.04%, $p<0.09$), albeit not significantly (Figure 5D and 5E).

EV-YF1 and CDC-exo modulate IL-10 expression

We have reported that EV-YF1 modulates IL-10 expression in BMDMs.[15] To test the hypothesis that EV-YF1 attenuates the effect of Ang II on cardiac hypertrophy by modulating IL-10 secretion, we measured IL-10 levels in plasma of mice infused with Ang

II 24 hours after the second injection of EV-YF1 or CDC-exo (day 16). At this time point, no differences in IL-10 levels were observed between mice infused with Ang II or saline. However, EV-YF1 did increase IL-10 levels relative to saline injection (1.8-fold, $p<0.01$, n=4) (Figure 6A). This observation demonstrates that EV-YF1 upregulates IL-10 levels in only 24 h. On the contrary, the second injection of CDC-exo seemed to lower plasma IL-10 levels compared to sham group (2.3-fold, $p<0.05$, n=4). At the end of the Ang II infusion (day 28), the profile of plasma IL-10 changed: IL-10 levels in the Ang II-infused group decreased modestly compared to sham, while those in EV-YF1 and CDC-exo groups were comparable to sham group (Figure 6B). At the end of the study (day 28), we analyzed tissue IL-10 levels in heart, spleen and kidney (Figures 6C-E). Cardiac IL-10 levels were significantly higher in Ang II-infused group than in sham (13.54 ± 1.285 (Ang II) vs. 9.496 ± 0.457 pg/mg protein (Sham), $p<0.05$, n=6-8). In contrast, levels of cardiac IL-10 in EV-YF1 and CDC-exo groups were similar to those in the sham group (Figure 6C). The same profile was observed for IL-10 levels in spleen (Figure 6D). IL-10 gene expression and IL-10-induced signaling pathways also play important roles in the regulation and maintenance of normal renal function. Indeed, IL-10 delivery slowed the functional decline in an animal model of chronic renal disease.[36] To establish whether the improved renal function was associated with higher levels of IL-10 in the kidney, we measured IL-10 levels in all experimental groups. A substantial decrease in IL-10 was observed in Ang II-infused group compared to sham (152 ± 3 (Ang II) vs. 243 ± 10 pg/mg protein (Sham), $p<0.001$, n=4). Interestingly, the EV-YF1 group showed similar levels to those in the sham group, significantly different from Ang II group (232 ± 12 pg/mg protein, $p<0.001$, n=4), while the CDC-exo group showed no difference with Ang II-infused group (Figure 6E).

Discussion

Here, we have shown that CDC-exo exert beneficial effects in a model of cardiac hypertrophy and renal injury induced by Ang II infusion. Moreover, we also demonstrated that EV-YF1, the most abundant RNA species in CDC-exo, itself recapitulates most of the beneficial effects of CDC-exo on CVD. We chose the Ang II infusion model as the renin–angiotensin system promotes hypertension, is a key mediator of cardiac adaptations to hemodynamic overload, and induces end organ damage including the heart and kidneys.[37] This model has direct clinical relevance as it emulates early stages in the progression of CVD. For EV-YF1 and CDC-exo administration, we opted for the retro-orbital route which is a reliable and consistent option for drug delivery in mice[38] and less invasive than previous intra-coronary or intra-myocardial injections used to deliver CDC-exo.[39] EV-YF1 and CDC-exo were injected at mid-course, when the cardiac hypertrophy phenotype was not yet pronounced, to test if the interventions could stop or attenuate the progression of cardiac remodeling and renal injury.

Both EV-YF1 and CDC-exo indeed attenuated the progression of cardiac hypertrophy. Cardiac mass assessed by echocardiography, heart-to-body weight ratio and expression of the fetal gene *Anp* were significantly decreased in EV-YF1 or CDC-exo groups compared to Ang II-infused mice. In most cases, these parameters reached values comparable to those in the sham group. These data are concordant with the observation of reduced cardiomyocyte size in mice exposed to EV-YF1 or CDC-exo, as well as attenuated Ang II-induced fibrosis.

Extending previous studies, we observed that CDC-exo[14, 31] and EV-YF1,[15] decreased the expression of pro-inflammatory cytokines *Il1b* and *Il6* in the heart, and blunted the expression of *CD68*, a marker of infiltrating cells. We demonstrated *in vitro* that EV-YF1 acts indirectly on cardiomyocytes and cardiac fibroblasts via regulation of the cytokine profile secreted by macrophages.[15] Indeed, attenuated effects of Ang II on *Anp* expression in cardiomyocytes or *Il6* in cardiac fibroblasts were only observed in the presence of BMDM-conditioned media overexpressing EV-YF1. As described by our group,[15] the secretion of IL-10 by BMDMs induced by EV-YF1 might counteract Ang II effects. These data add to our previous finding showing a direct role of EV-YF1 on macrophage polarization, and underline the importance of communication among different cell types during cardiac repair.[40]

Our previous studies have shown beneficial effects of CDC-exo which extend beyond the heart; for example, skeletal muscle function and structure improved after CDC-exo administration in the *mdx* mouse model of muscular dystrophy.[41] Here we demonstrated that both CDC-exo and their most abundant small RNA species, EV-YF1, exert beneficial effects on kidney. The kidney is a key target of Ang II, and prolonged Ang II infusion leads to renal dysfunction.[42] Here, we have shown that EV-YF1 or CDC-exo decrease tubulointerstitial fibrosis, mesangial expansion and proteinuria. In addition, EV-YF1 or CDC-exo decreased expression levels of NGAL, a biomarker of renal injury used in patients with HF to estimate the risk of worsening renal function.[34] Inflammation is a common feature of many pathological conditions including cardiac hypertrophy, myocardial infarction, and renal disease. Interestingly, CDC-exo and/or EV-YF1[15, 31, 41] have demonstrated beneficial effects in many of these pathological conditions. Thus, the anti-inflammatory effects of CDC-exo and EV-YF1 might rationalize why these interventions are effective in multiple target organs.

The beneficial effects of EV-YF1 and CDC-exo occur without modifying blood pressure. *In vitro* studies have shown that, besides its hemodynamic actions, Ang II also exerts direct trophic effects on cardiac and different renal cell types by promoting structural remodeling and cell proliferation[43] independently of hypertension.[44, 45] Our studies are consistent with the idea that EV-YF1 and CDC-exo prevent cardiac hypertrophy and ameliorate renal injury by blocking local actions of Ang II on target tissues, independently of the hemodynamic effects of Ang II. The high expression of EV-YF1 in heart after systemic injection seems to facilitate actions at this site of injury, potentially via cardiac-resident macrophages. On the other hand, high expression in the spleen, which can mobilize numerous monocytes in response to injury,[46] may reflect an early action of EV-YF1 on splenic macrophages. EV-YF1 might induce a rapid activation of splenic macrophages to produce high levels of IL-10, which then counterbalance inflammation in heart and kidney. This could explain the low renal EV-YF1 expression after injection. We have established that EV-YF1 increased plasma IL-10 levels within just 24 hours after retro-orbital injection, and these levels were sustained during intervention, while animals not exposed to EV-YF1 showed lower plasma IL-10 levels at the end of the 28 days of Ang II-infusion.[47] CDC-exo also increased IL-10 levels in a delayed manner compared to EV-YF1. Plasma levels of IL-10 in the EV-YF1 group were similar to those in sham. The normal IL-10 plasma levels correlate with normal levels in heart, spleen and kidney. We speculate that high levels of plasma IL-10, observed after the

first injections of EV-YF1, arise from splenic macrophages homing to sites of injuries in heart and kidney, and counterbalance the progression of the inflammatory state in these organs (Figure S6 in the online-only Data Supplement. In contrast, during Ang II infusion, the persistent cardiac inflammation requires a permanent production of IL-10 as a compensatory effect[27] that explains the high levels of IL-10 in heart and splenic tissues in Ang II-infused animals. More experiments would be required, however, to test these hypotheses.

The mechanism of action on the kidney appeared somewhat different than that in the heart, given that EV-YF1 maintained IL-10 levels that were reduced upon Ang II-infusion. IL-10, produced by mesangial cells, plays an important role in normal renal physiology, as well as during acute kidney injury, and in the progression of chronic renal failure.[48] Under some conditions, IL-10 has a protective effect reducing kidney injury, with lower proteinuria and reductions in glomerulosclerosis and interstitial fibrosis.[36, 49] The data support the notion that EV-YF1 improves kidney function by modulating IL-10 levels, while CDC-exo actions cannot be explained that simply. Indeed, EV-YF1 restored normal levels of IL-10 in kidney while CDC-exo animals showed levels comparable to those in the Ang II group.

Perspectives

EV-YF1 or CDC-exo attenuate LV remodeling and improve kidney function in a murine hypertensive model. The study was designed to test only early-stage disease. We do not yet know whether such interventions, if initiated after the pathology is fully established, would be able to reverse cardiac hypertrophy and kidney dysfunction. We also demonstrated that EV-YF1 and CDC-exo re-established normal levels of IL-10 in heart, kidney and spleen after Ang II infusion. Some, but not all, of the benefits are associated with directionally-appropriate changes in IL-10, but additional interventions (e.g., using a neutralizing antibody against IL-10) would be required to strengthen the evidence for a cause-and-effect relationship. Although IL-10 treatment appears beneficial in heart failure following myocardial infarction and cardiac hypertrophy,[50, 51] the high cost-benefit ratio for an appropriate dose of IL-10 to achieve a therapeutic effect in humans has limited its translation to clinical practice.[52] Intravenous treatment with EV-YF1 or CDC-exo may recapitulate the beneficial effects of IL-10 without the associated limitations. Indeed, CDC-exo and EV-YF1 could represent new classes of therapeutic agents: the former are cell-produced vesicles with multiple bioactive contents, while the latter is a single defined biological constituent of those vesicles. Both act directly to mitigate end organ damage, independently of blood pressure regulation.

Supplementary Material

Refer to Web version on PubMed Central for supplementary material.

Acknowledgments

Sources of Funding

This work was supported by NIH R01 HL124074 and the Board of Governors of the Cedars-Sinai Medical Center to EM, CIRM DISC1 NH-W0005A-LA to LC, and AHA Scientist Development Grant 16SDG30130015 to JFG.

References

1. Benjamin EJ, Blaha MJ, Chiuve SE, Cushman M, Das SR, Deo R, et al. Heart disease and stroke statistics—2017 update: A report from the american heart association. Circulation. 2017; 135:e146–e603. [PubMed: 28122885]
2. Bernardo BC, Weeks KL, Pretorius L, McMullen JR. Molecular distinction between physiological and pathological cardiac hypertrophy: Experimental findings and therapeutic strategies. Pharmacol Ther. 2010; 128:191–227. [PubMed: 20438756]
3. Porrello ER, D'Amore A, Curl CL, Allen AM, Harrap SB, Thomas WG, et al. Angiotensin ii type 2 receptor antagonizes angiotensin ii type 1 receptor-mediated cardiomyocyte autophagy. Hypertension. 2009; 53:1032–1040. [PubMed: 19433781]
4. Rothermel BA, Hill JA. Myocyte autophagy in heart disease: Friend or foe? Autophagy. 2007; 3:632–634. [PubMed: 17786025]
5. Heineke J, Molkentin JD. Regulation of cardiac hypertrophy by intracellular signalling pathways. Nat Rev Mol Cell Biol. 2006; 7:589–600. [PubMed: 16936699]
6. Liu M, Li XC, Lu L, Cao Y, Sun RR, Chen S, et al. Cardiovascular disease and its relationship with chronic kidney disease. Eur Rev Med Pharmacol Sci. 2014; 18:2918–2926. [PubMed: 25339487]
7. Smith RR, Barile L, Cho HC, Leppo MK, Hare JM, Messina E, et al. Regenerative potential of cardiosphere-derived cells expanded from percutaneous endomyocardial biopsy specimens. Circulation. 2007; 115:896–908. [PubMed: 17283259]
8. Makkar RR, Smith RR, Cheng K, Malliaras K, Thomson LE, Berman D, et al. Intracoronary cardiosphere-derived cells for heart regeneration after myocardial infarction (caduceus): A prospective, randomised phase 1 trial. Lancet. 2012; 379:895–904. [PubMed: 22336189]
9. Malliaras K, Li TS, Luthringer D, Terrovitis J, Cheng K, Chakravarty T, et al. Safety and efficacy of allogeneic cell therapy in infarcted rats transplanted with mismatched cardiosphere-derived cells. Circulation. 2012; 125:100–112. [PubMed: 22086878]
10. Kreke M, Smith RR, Marban L, Marban E. Cardiospheres and cardiosphere-derived cells as therapeutic agents following myocardial infarction. Expert Rev Cardiovasc Ther. 2012; 10:1185–1194. [PubMed: 23098154]
11. Tseliou E, Pollan S, Malliaras K, Terrovitis J, Sun B, Galang G, et al. Allogeneic cardiospheres safely boost cardiac function and attenuate adverse remodeling after myocardial infarction in immunologically mismatched rat strains. Journal of the American College of Cardiology. 2013; 61:1108–1119. [PubMed: 23352785]
12. Tseliou E, Reich H, de Couto G, Terrovitis J, Sun B, Liu W, et al. Cardiospheres reverse adverse remodeling in chronic rat myocardial infarction: Roles of soluble endoglin and tgf-beta signaling. Basic Res Cardiol. 2014; 109:443. [PubMed: 25245471]
13. de Couto G, Liu W, Tseliou E, Sun B, Makkar N, Kanazawa H, et al. Macrophages mediate cardioprotective cellular postconditioning in acute myocardial infarction. J Clin Invest. 2015; 125:3147–3162. [PubMed: 26214527]
14. Ibrahim Ahmed G-E, Cheng K, Marbán E. Exosomes as critical agents of cardiac regeneration triggered by cell therapy. Stem Cell Reports. 2014; 2:606–619. [PubMed: 24936449]
15. Cambier L, de Couto G, Ibrahim A, Echavez AK, Valle J, Liu W, et al. Y rna fragment in extracellular vesicles confers cardioprotection via modulation of il-10 expression and secretion. EMBO Mol Med. 2017; 9:337–352. [PubMed: 28167565]
16. Hendrick JP, Wolin SL, Rinke J, Lerner MR, Steitz JA. Ro small cytoplasmic ribonucleoproteins are a subclass of la ribonucleoproteins: Further characterization of the ro and la small ribonucleoproteins from uninfected mammalian cells. Molecular and Cellular Biology. 1981; 1:1138–1149. [PubMed: 6180298]
17. Lerner MR, Boyle JA, Hardin JA, Steitz JA. Two novel classes of small ribonucleoproteins detected by antibodies associated with lupus erythematosus. Science. 1981; 211:400–402. [PubMed: 6164096]
18. Teunissen SWM, Kruithof MJM, Farris AD, Harley JB, Venrooij WJv, Pruijn GJM. Conserved features of y rnas: A comparison of experimentally derived secondary structures. Nucleic Acids Research. 2000; 28:610–619. [PubMed: 10606662]

19. Hogg JR, Collins K. Human y5 rna specializes a ro ribonucleoprotein for 5s ribosomal rna quality control. Genes & development. 2007; 21:3067–3072. [PubMed: 18056422]
20. Zhang AT, Langley AR, Christov CP, Kheir E, Shafee T, Gardiner TJ, et al. Dynamic interaction of y rnas with chromatin and initiation proteins during human DNA replication. Journal of Cell Science. 2011; 124:2058–2069. [PubMed: 21610089]
21. Röther S, Meister G. Small rnas derived from longer non-coding rnas. Biochimie. 2011; 93:1905–1915. [PubMed: 21843590]
22. Hall Adam E, Dalmay T. Discovery of novel small rnas in the quest to unravel genome complexity. Biochemical Society Transactions. 2013; 41:866–870. [PubMed: 23863146]
23. Vojtech L, Woo S, Hughes S, Levy C, Ballweber L, Sauteraud RP, et al. Exosomes in human semen carry a distinctive repertoire of small non-coding rnas with potential regulatory functions. Nucleic Acids Research. 2014; 42:7290–7304. [PubMed: 24838567]
24. Lunavat TR, Cheng L, Kim DK, Bhadury J, Jang SC, Lasser C, et al. Small rna deep sequencing discriminates subsets of extracellular vesicles released by melanoma cells–evidence of unique microrna cargos. RNA Biol. 2015; 12:810–823. [PubMed: 26176991]
25. Dhahbi JM, Spindler SR, Atamna H, Boffelli D, Martin DI. Deep sequencing of serum small rnas identifies patterns of 5′ trna half and yrna fragment expression associated with breast cancer. Biomark Cancer. 2014; 6:37–47. [PubMed: 25520563]
26. Crowley SD, Gurley SB, Herrera MJ, Ruiz P, Griffiths R, Kumar AP, et al. Angiotensin ii causes hypertension and cardiac hypertrophy through its receptors in the kidney. Proc Natl Acad Sci U S A. 2006; 103:17985–17990. [PubMed: 17090678]
27. Kwon WY, Cha HN, Heo JY, Choi JH, Jang BI, Lee IK, et al. Interleukin-10 deficiency aggravates angiotensin ii-induced cardiac remodeling in mice. Life Sci. 2016; 146:214–221. [PubMed: 26775566]
28. Gray MO, Long CS, Kalinyak JE, Li HT, Karliner JS. Angiotensin ii stimulates cardiac myocyte hypertrophy via paracrine release of tgf-beta 1 and endothelin-1 from fibroblasts. Cardiovasc Res. 1998; 40:352–363. [PubMed: 9893729]
29. Wang Y, Li Y, Wu Y, Jia L, Wang J, Xie B, et al. 5tnf-alpha and il-1beta neutralization ameliorates angiotensin ii-induced cardiac damage in male mice. Endocrinology. 2014; 155:2677–2687. [PubMed: 24877626]
30. Jia L, Li Y, Xiao C, Du J. Angiotensin ii induces inflammation leading to cardiac remodeling. Front Biosci (Landmark Ed). 2012; 17:221–231. [PubMed: 22201740]
31. de Couto G, Gallet R, Cambier L, Jaghatspanyan E, Makkar N, Dawkins JF, et al. Exosomal microrna transfer into macrophages mediates cellular postconditioning. Circulation. 2017; 136:200–214. [PubMed: 28411247]
32. Johnston BM, Owen DA. Tissue blood flow and distribution of cardiac output in cats: Changes caused by intravenous infusions of histamine and histamine receptor agonists. Br J Pharmacol. 1977; 60:173–180. [PubMed: 880428]
33. Ma F, Li Y, Jia L, Han Y, Cheng J, Li H, et al. Macrophage-stimulated cardiac fibroblast production of il-6 is essential for tgf beta/smad activation and cardiac fibrosis induced by angiotensin ii. PLoS One. 2012; 7:e35144. [PubMed: 22574112]
34. Bolignano D, Lacquaniti A, Coppolino G, Donato V, Campo S, Fazio MR, et al. Neutrophil gelatinase-associated lipocalin (ngal) and progression of chronic kidney disease. Clin J Am Soc Nephrol. 2009; 4:337–344. [PubMed: 19176795]
35. Guo F, Chen XL, Wang F, Liang X, Sun YX, Wang YJ. Role of angiotensin ii type 1 receptor in angiotensin ii-induced cytokine production in macrophages. J Interferon Cytokine Res. 2011; 31:351–361. [PubMed: 21235392]
36. Mu W, Ouyang X, Agarwal A, Zhang L, Long DA, Cruz PE, et al. Il-10 suppresses chemokines, inflammation, and fibrosis in a model of chronic renal disease. J Am Soc Nephrol. 2005; 16:3651–3660. [PubMed: 16251240]
37. Reid IA, Morris BJ, Ganong WF. The renin-angiotensin system. Annu Rev Physiol. 1978; 40:377–410. [PubMed: 205167]

38. Steel CD, Stephens AL, Hahto SM, Singletary SJ, Ciavarra RP. Comparison of the lateral tail vein and the retro-orbital venous sinus as routes of intravenous drug delivery in a transgenic mouse model. Lab Anim (NY). 2008; 37:26–32. [PubMed: 18094699]
39. Gallet R, Dawkins J, Valle J, Simsolo E, de Couto G, Middleton R, et al. Exosomes secreted by cardiosphere-derived cells reduce scarring, attenuate adverse remodelling, and improve function in acute and chronic porcine myocardial infarction. Eur Heart J. 2017; 38:201–211. [PubMed: 28158410]
40. Frangogiannis NG. Inflammation in cardiac injury, repair and regeneration. Curr Opin Cardiol. 2015; 30:240–245. [PubMed: 25807226]
41. Aminzadeh MA, , Rogers RG, , Gouin K, , Fournier M, , Tobin RE, , Guan X. , et al. Reversal of cardiac and skeletal manifestations of duchenne muscular dystrophy by cardiosphere-derived cells and their exosomes in mdx dystrophic mice and in human duchenne cardiomyocytes. bioRxiv web site https://www.biorxiv.org/content/early/2017/04/20/128900. Accessed April 13, 2018
42. Kobori H, Nangaku M, Navar LG, Nishiyama A. The intrarenal renin-angiotensin system: From physiology to the pathobiology of hypertension and kidney disease. Pharmacol Rev. 2007; 59:251–287. [PubMed: 17878513]
43. Wolf G, Jablonski K, Schroeder R, Reinking R, Shankland SJ, Stahl RA. Angiotensin ii-induced hypertrophy of proximal tubular cells requires p27kip1. Kidney Int. 2003; 64:71–81. [PubMed: 12787397]
44. Mazzolai L, Nussberger J, Aubert JF, Brunner DB, Gabbiani G, Brunner HR, et al. Blood pressure-independent cardiac hypertrophy induced by locally activated renin-angiotensin system. Hypertension. 1998; 31:1324–1330. [PubMed: 9622149]
45. Anderson PW, Do YS, Hsueh WA. Angiotensin ii causes mesangial cell hypertrophy. Hypertension. 1993; 21:29–35. [PubMed: 8418021]
46. Swirski FK, Nahrendorf M, Etzrodt M, Wildgruber M, Cortez-Retamozo V, Panizzi P, et al. Identification of splenic reservoir monocytes and their deployment to inflammatory sites. Science. 2009; 325:612–616. [PubMed: 19644120]
47. Miguel-Carrasco JL, Zambrano S, Blanca AJ, Mate A, Vazquez CM. Captopril reduces cardiac inflammatory markers in spontaneously hypertensive rats by inactivation of nf-kb. J Inflamm (Lond). 2010; 7:21. [PubMed: 20462420]
48. Sinuani I, Averbukh Z, Gitelman I, Rapoport MJ, Sandbank J, Albeck M, et al. Mesangial cells initiate compensatory renal tubular hypertrophy via il-10-induced tgf-beta secretion: Effect of the immunomodulator as101 on this process. Am J Physiol Renal Physiol. 2006; 291:F384–394. [PubMed: 16571592]
49. Jin Y, Liu R, Xie J, Xiong H, He JC, Chen N. Interleukin-10 deficiency aggravates kidney inflammation and fibrosis in the unilateral ureteral obstruction mouse model. Lab Invest. 2013; 93:801–811. [PubMed: 23628901]
50. Krishnamurthy P, Rajasingh J, Lambers E, Qin G, Losordo DW, Kishore R. Il-10 inhibits inflammation and attenuates left ventricular remodeling after myocardial infarction via activation of stat3 and suppression of hur. Circ Res. 2009; 104:e9–18. [PubMed: 19096025]
51. Verma SK, Krishnamurthy P, Barefield D, Singh N, Gupta R, Lambers E, et al. Interleukin-10 treatment attenuates pressure overload-induced hypertrophic remodeling and improves heart function via signal transducers and activators of transcription 3-dependent inhibition of nuclear factor-kappab. Circulation. 2012; 126:418–429. [PubMed: 22705886]
52. Asadullah K, Sterry W, Volk HD. Interleukin-10 therapy–review of a new approach. Pharmacol Rev. 2003; 55:241–269. [PubMed: 12773629]

Novelty and Significance

What Is New?

- CDC-exo and the small non-coding RNA fragment, EV-YF1 exert beneficial effects in heart and kidney of hypertensive mice.
- The beneficial effects of CDC-exo and EV-YF1 are independent of blood pressure regulation.

What Is Relevant?

- Intravenous administration of EV-YF1 or CDC-exo represent efficient therapeutic approaches to target organs affected by hypertension.
- Unlike RAS blockers or beta-blockers, EV-YF1 or CDC-exo benefits on the heart and kidney are independent of blood pressure.
- EV-YF1, by modulating *Il10* expression, could represent a new therapeutic approach for attenuation of end-organ injury in hypertension.

Summary

Exposure to EV-YF1 or CDC-exo significantly attenuates LV remodeling and renal injury induced by Ang II infusion. EV-YF1 or CDC-exo reduce cardiac hypertrophy, fibrosis and inflammation. In addition, either entity also decreases renal inflammation and fibrosis, while and ameliorating kidney injury. Modulation of the anti-inflammatory cytokine IL-10 may underlie some of these beneficial effects, but further work is required to establish a cause-and-effect relationship.

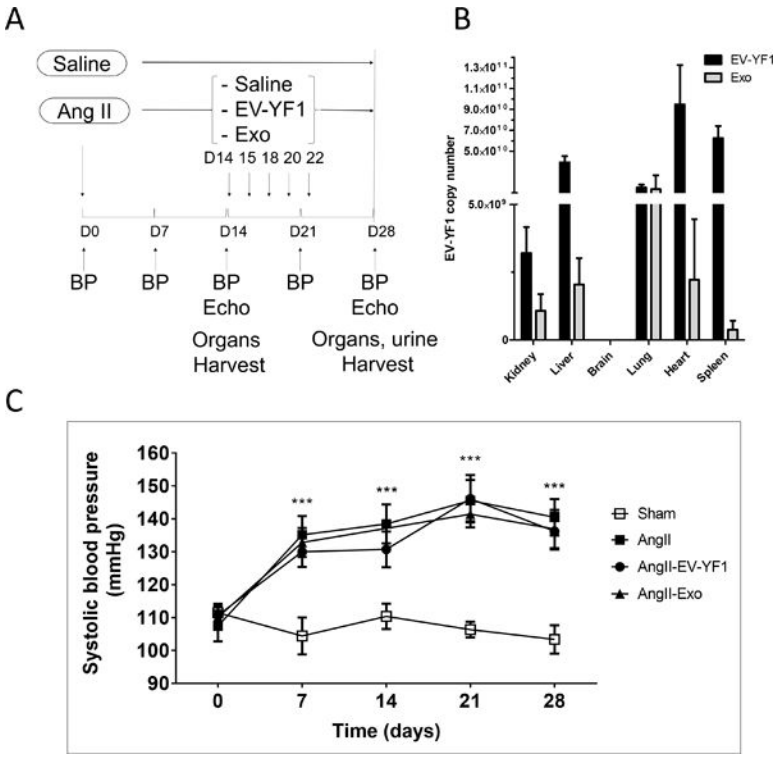

Figure 1. EV-YF1 and CDC-exo biodistribution after retro-orbital injection in an Ang II-infused mouse

A, Study design of Ang II infusion with EV-YF1 and CDC-exo treatment. **B**, EV-YF1 copy number by qPCR representing the distribution of EV-YF1 and CDC-exo 24 h after retro-orbital injection. (No expression was detected in brain). Values are means ± SEM; n = 4 animals/group. **C**, Systolic blood pressure (SBP) was recorded by tail-cuff in mice before and after chronic subcutaneous infusion of Ang II or saline (sham) weekly for 28 days. Chronic infusion of Ang II significantly increased SBP independently of EV-YF1 or CDC-exo treatment. Values are means ± SEM; n = 5 animals/group. Groups were compared using 1-way ANOVA followed by Tukey's multiple comparisons test; ***P < 0.001 between sham vs. all the groups at every time points except baseline.

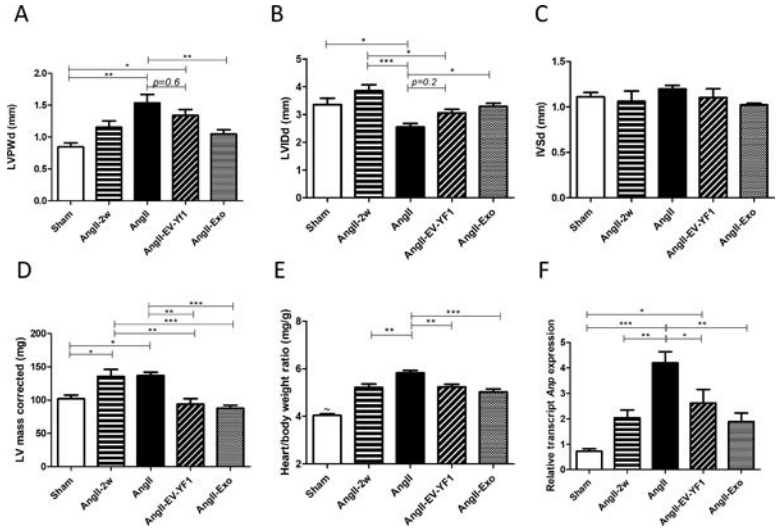

Figure 2. Effect of EV-YF1 and CDC-exo treatment on cardiac function and hypertrophy

Cardiac morphology (**A-D**) were assessed by echocardiography at 2 weeks (AngII-2w) and 28 days after saline (sham) or Ang II infusion (AngII). Additional groups of mice were treated with Ang II plus EV-YF1 (AngII-EV-YF1) or Ang II plus CDC-exo (AngII-Exo). LVPWd: LV posterior wall thickness, end-diastole; LVIDd: LV internal diastolic diameter; IVSd: interventricular septal thickness, end-diastole. Values are means ± SEM; n = 5-10 animals/group. **E**, heart weight-to-body weight ratio. Values are means ± SEM; n = 7-10 animals/group. ~P<0.001 between sham and all the groups. **F**, relative expression of cardiac *Anp* by qPCR. Values are means ± SEM; n = 5 animals/group. Groups were compared using 1-way ANOVA followed by Tukey's multiple comparisons test; *P < 0.05, **P < 0.01, ***P < 0. 001.

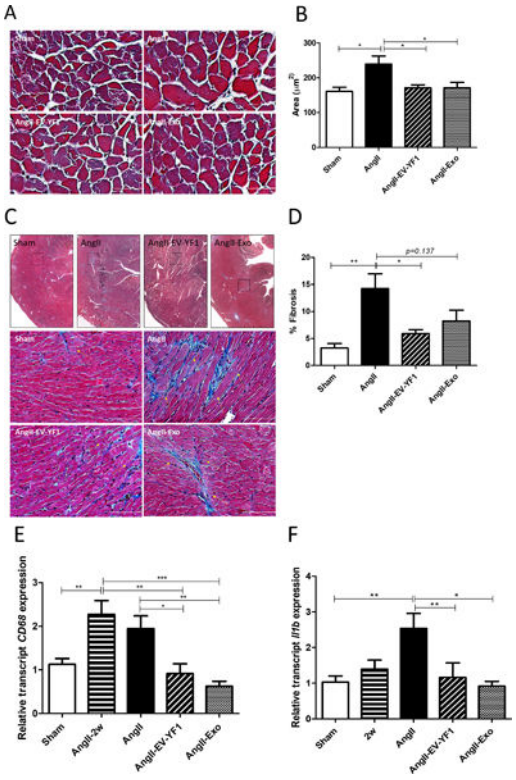

Figure 3. EV-YF1 and CDC-exo treatment decrease Ang II-induced cardiac hypertrophy, fibrosis and inflammation

A, micrographs (magnification: ×20) showing representative cross-sectional area of cardiac myocytes stained with Masson's trichrome of mice that received subcutaneous infusion of saline or Ang II for 28 days treated with saline, EV-YF1 or CDC-exo. **B**, quantitative measurements of cross-sectional area of myocytes within transverse cardiac sections. Graph depicts the mean ± SEM; n = 4 animals/group. Scale bars = 25 μm. **C**, upper panel, micrographs (magnification: 4×) showing interstitial LV fibrosis in myocardial sections stained with Masson's trichrome, squares delimit regions represented in higher magnification (×20) in lower panel, yellow arrows show interstitial myocardial fibrosis. **D**, quantitative measurements of interstitial myocardial fibrosis within cardiac sections. Data are means ± SEM; n = 3 animals/group. Scale bars = 50 μm. **E-F**, gene expression of *CD68* in **E** and *Il1b* in **F** in heart tissue from mice that received subcutaneous infusion of Ang II for 2 weeks (AngII-2w) and for 28 days of saline or Ang II treated with saline, EV-YF1 or CDC-exo, as determined by qPCR. Graphs depict the mean ± SEM; n = 7-10 animals/group. Groups were compared using 1-way ANOVA followed by Tukey's multiple comparisons test; *P < 0.05, **P < 0.01, ***P < 0.001.

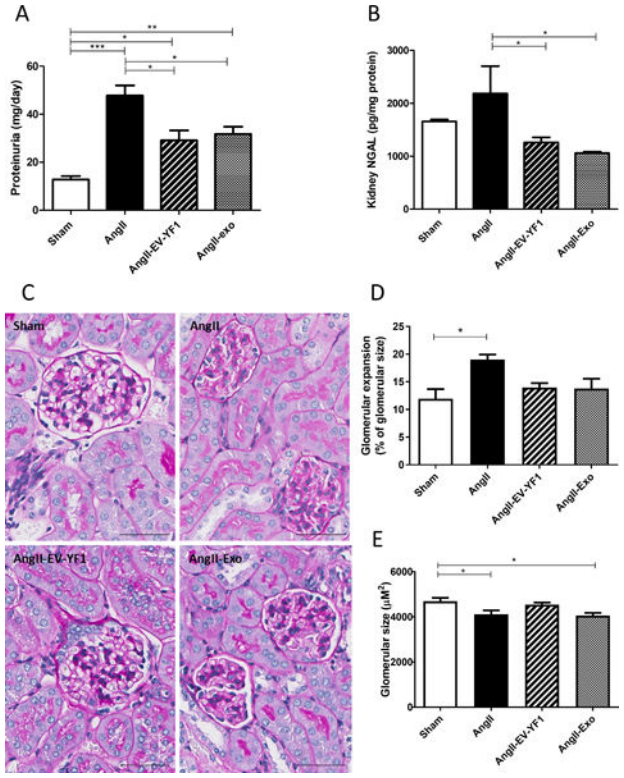

Figure 4. EV-YF1 and CDC-exo treatment decrease Ang II-induced kidney dysfunction

Proteinuria in **A** and NGAL levels in kidney in **B** as determined by ELISA. Graphs depict the mean ± SEM; n = 4 animals/group. **C**, micrographs (magnification: ×20) showing representative glomerular expansion and size in renal sections stained with Periodic acid-Schiff (PAS). Quantitative measurements of glomerular expansion in **D** and size in **E** of 20 glomeruli within renal sections. Data are means ± SEM; n = 4 animals/group. Scale bars = 50 µm. Groups were compared using 1-way ANOVA followed by Tukey's multiple comparisons test; *P < 0.05, **P < 0.01, ***P < 0.001.

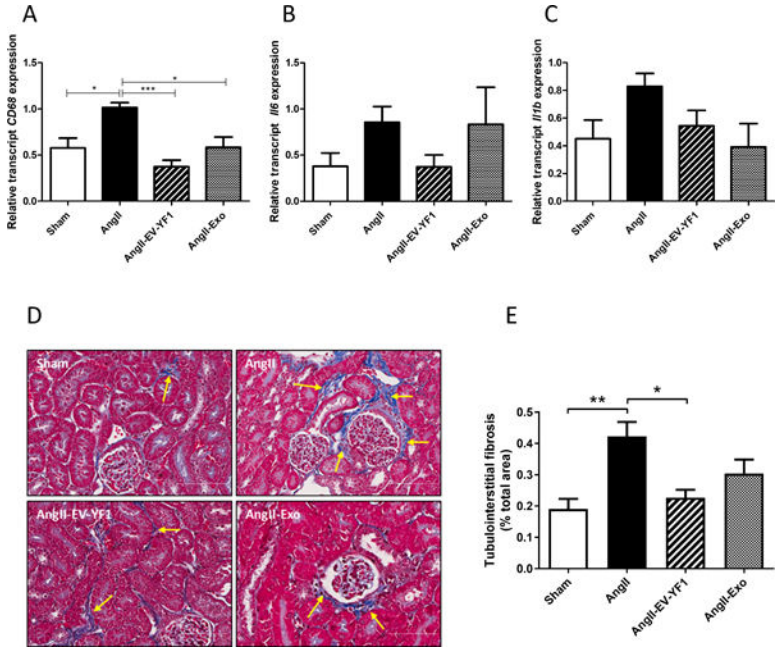

Figure 5. EV-YF1 and CDC-exo treatment decrease Ang II-induced kidney inflammation and fibrosis

A-C, gene expression of *CD68* in **A**, *Il16* in **B** and *Il1b* in **C** in kidney tissue from mice that received subcutaneous infusion of Ang II for 28 days of saline or Ang II treated with saline, EV-YF1 or CDC-exo, as determined by qPCR. Graphs depict the mean ± SEM; n = 5 animals/group. **D**, micrographs (magnification: ×20) showing representative tubulointerstitial fibrosis (arrows) in kidney sections stained with Masson's trichrome. **E**, Quantitative measurements of tubulointerstitial fibrosis within kidney sections. Data are means ± SEM; n = 5 animals/group. Scale bars = 70 μm. Groups were compared using 1-way ANOVA followed by Tukey's multiple comparisons test; *P < 0.05, **P < 0.01, ***P < 0.001.

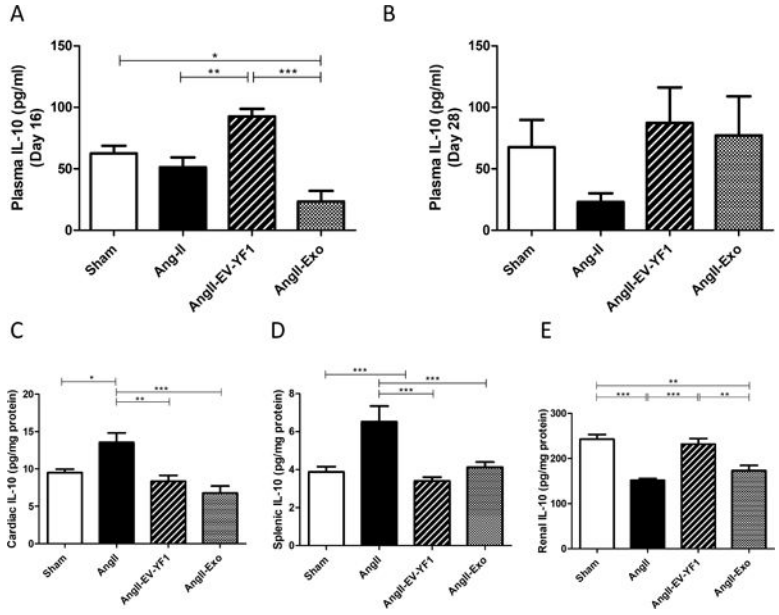

Figure 6. EV-YF1 and CDC-exo modulate IL-10 expression

A, Plasma levels of IL-10 at day 16 of the study (*ie*: 24 h after the second injection of saline, EV-YF1 or CDC-exo in mice infused with Ang II), as determined by ELISA. Graph depicts the mean ± SEM; n = 4-5 animals/group. **B-E**, Plasma in **B**, cardiac in **C**, splenic in **D** and renal in **E** levels of IL-10 at the final day (day 28) of the study in mice that received subcutaneous infusion of saline or Ang II for 28 days treated with saline, EV-YF1 or CDC-exo, as determined by ELISA. Graphs depict the mean ± SEM; n = 5-9 animals/group. Groups were compared using 1-way ANOVA followed by Tukey's multiple comparisons test; *P < 0.05, **P < 0.01, ***P < 0.001.